DOI: 10.1002/ejic.200500778

Platinum-Group Chelate Complexes with 9-Hydroxyphenalenone Derivatives: Synthesis, Structures, Spectroscopic Properties and Cytotoxic Activities

Tomoyuki Mochida,*[a,b] Reiko Torigoe,[a] Takeo Koinuma,[a] Chika Asano,[a] Tadaaki Satou,[c] Kazuo Koike,[c] and Tamotsu Nikaido[c]

Keywords: Platinum / Rhodium / Palladium / O ligands / Metal–metal interactions

The following platinum-group chelate complexes with 5-R-9-hydroxyphenalenone (L^1: R = H; L^2: R = Me; L^3: R = Pr) have been prepared: $[Rh^I(L)(CO)_2]$ (**1a**: L = L^1; **1b**: L = L^2; **1c**: L = L^3), $[Pd^{II}(L)_2]$ (**2a**: L = L^2; **2b**: L = L^3), $[Pt^{II}(L^1)(NH_3)_2](NO_3)$ (**3**), and $(Bu_4N)[Pt^{II}(L^1)(Cl)_2]$ (**4**). Compounds **1a** and **1b** are different colors in the solid state: yellow and deep red, respectively. X-ray analysis revealed that **1a** has a regular π–π stacking structure while **1b** has a dimer-like arrangement with a Rh^I–Rh^I distance of 3.2336(6) Å. Both solids were luminescent at 77 K. Compounds **2a** and **2b** are planar extended π-conjugated complexes, which exhibit two-dimensional stacking modes in the crystal. The solid-state structure of complex **3** is hydrogen-bonded in a polar arrangement. The cytotoxic activities of **1a**, **3**, and **4**, evaluated in vitro against HL60 human acute myeloid leukemia cell lines, were comparable to that of cisplatin.

Introduction

Platinum-group metal complexes with various ligands have attracted growing attention in recent decades because of their unique photochemical[1] and electronic properties.[2] Here we report the use of hydroxyphenalenone as an extended π-conjugated ligand to explore a novel type of complex. The phenalenyl system is an odd-alternant hydrocarbon,[3,4] the unique properties of which have been widely investigated. Haddon has reported the interesting properties of spiro-biphenalenyl radicals, which exhibit electronic-switching phenomena in the solid state.[5] Several transition-metal complexes of phenalenyl derivatives have been reported: a neutral palladium complex with a η^3-phenalenyl ligand was prepared by Nakasuji,[6] and some transition-metal complexes with phenalenone-related ligands were prepared in the 1970s.[7,8] More recently, metal chelate complexes with 9-hydroxyphenalenones have been prepared, including aluminum complexes for multilayer light-emitting devices[9] and a luminescent europium complex.[10] However, no examples of phenalenone chelate complexes with platinum-group metals have been reported. We are interested in the antitumor potential of such complexes because their planar π-conjugated nature might allow intercalation into DNA to enhance cytotoxic activity.

In this study, we prepared chelate complexes of platinum-group metals with 9-hydroxyphenalenone (HL^1), its 5-methyl derivative (HL^2), and a 5-propyl derivative (HL^3) (Scheme 1). Use of the 5-alkyl derivatives improved the solubility of the complexes. We also tried, unsuccessfully, to prepare a 5-*tert*-butyl ligand by a Friedel–Crafts or similar condensation reaction. Here we report the preparation and properties of $[Rh^I(L)(CO)_2]$ (**1a**: L = L^1; **1b**: L = L^2; **1c**: L = L^3), $[Pd^{II}(L)_2]$ (**2a**: L = L^2; **2b**: L = L^3), $[Pt^{II}(L^1)(NH_3)_2](NO_3)$ (**3**), and $(Bu_4N)[Pt^{II}(L^1)(Cl)_2]$ (**4**). The molecular structures were confirmed crystallographically, and the remarkable difference in color between **1a** and **1b** was rationalized in terms of metal–metal interactions. Furthermore, the cytotoxic activities of **1a**, **3**, and **4** against human acute myeloid leukemia cells were evaluated.

Results and Discussion

Preparation and Spectroscopic Properties

Reaction of the 9-hydroxyphenalenone derivatives (HL^1, HL^2, and HL^3) with various metal sources in the presence of base produced chelate complexes (Scheme 1). We prepared the neutral complexes **1a**–**c** and **2a**–**b**, the anionic complex **3**, and the cationic complex **4** using methods analogous to the known preparations of chelate complexes of platinum-group metals with acetylacetonate derivatives.[11–15] We could not obtain platinum analogs of **2**; similar procedures afforded uncharacterizable black precipi-

[a] Department of Chemistry, Faculty of Science, Toho University, Miyama, Funabashi, Chiba 274-8510, Japan
Fax: +81-47-472-4406
E-mail: mochida@chem.sci.toho-u.ac.jp
[b] Research Center for Materials with Integrated Properties, Toho University,
Miyama, Funabashi, Chiba 274-8510, Japan
[c] Department of Pharmacognosy, Faculty of Pharmaceutical Sciences, Toho University,
Miyama, Funabashi, Chiba 274-8510, Japan
Supporting information for this article is available on the WWW under http://www.eurjic.org or from the author.

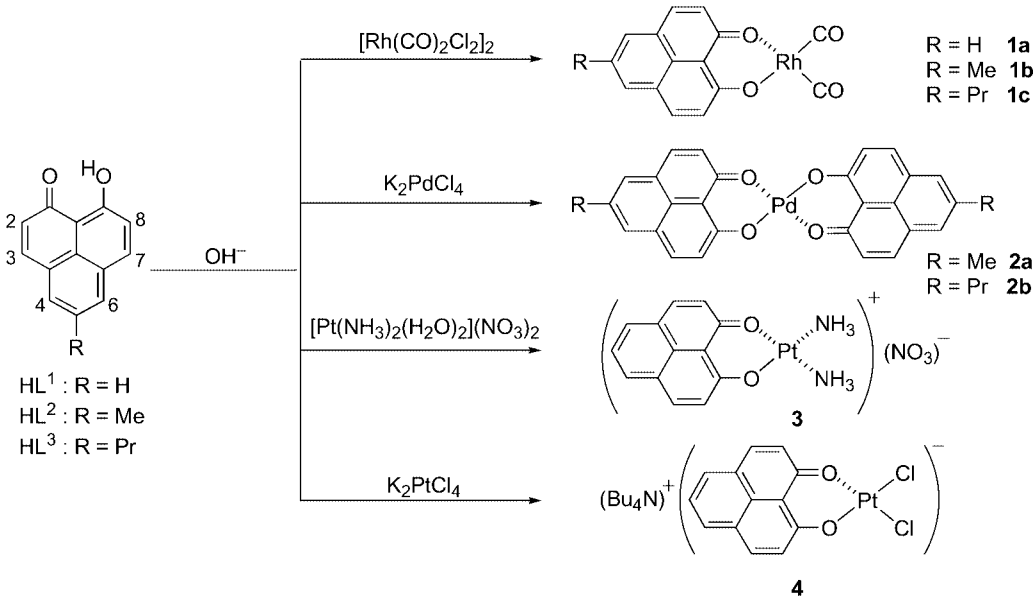

Scheme 1.

tates. Attempted syntheses of Magnus-type complexes using **3** and **4** failed.

The ^{1}H NMR spectroscopic data for compounds **1**–**4** are listed in Table 1 alongside the infrared stretching frequencies of C=O and other characteristic vibrations. In **1a**–**c** and **2b**, the signals for H^2 and H^4 exhibited downfield shifts, while H^3 was shifted upfield relative to their free ligand values. In **3** and **4**, the ring protons showed slight upfield shifts. The ligand C=O stretching bands were observed at frequencies slightly lower than those of the free ligand. In DMF solution, the lowest energy UV/Vis absorption bands for HL^1, HL^2, and HL^3 appeared at λ_{max} = 449, 449, and 438 nm, respectively. The lowest energy absorption bands for the metal complexes were found at lower energies than those of the ligands: λ_{max} = 498 (**2a**), 497 (**2b**), 477 (**3**), and 461 nm (**4**) in DMF, and at around λ_{max} = 460 nm for **1a**–**c** in dichloromethane. Compounds **1a**–**c** decomposed[16] when heated in DMF or DMSO.

In the following sections, the structures and solid-state properties of the individual complexes are described. Crystal data, data collection parameters, and analysis statistics are listed in Table 2, and selected bond lengths and bond angles given in Table 3. ORTEP[17] drawings of the molecular structures of **1a**, **2a**, **3**, and **4**, as well as the packing diagrams of **2b** and **4**, have been deposited as supporting information.

[Rh^I(L^1)(CO)$_2$] (1a) and [Rh^I(L^2)(CO)$_2$] (1b)

The rhodium ion in these complexes is coordinated by the phenalenone ligand and two CO ligands in a square planar arrangement. The molecular geometries of **1a** and

Table 1. ^{1}H NMR chemical shifts [ppm] and IR stretching frequencies [cm^{-1}] for ligands and complexes **1**–**4**.

Comp.	^{1}H NMR[a] Solvent	H2, H8 ($J_{H,H}$)	H3, H7 ($J_{H,H}$)	H4, H6 ($J_{H,H}$)	R ($J_{H,H}$)	IR[b] ν(C=O)
HL^1	$CDCl_3$	7.19 (9.16 Hz)	8.11 (9.80 Hz)	8.03 (9.16 Hz)	7.61 [R = H] (7.64 Hz)	1585, 1633
HL^1	[D$_6$]DMSO	7.24 (9.16 Hz)	8.41 (9.16 Hz)	8.30 (7.32 Hz)	7.74 [R = H] (7.64 Hz)	
1a	$CDCl_3$	7.33 (9.16 Hz)	8.08 (9.16 Hz)	8.06 (7.32 Hz)	7.61 [R = H] (7.62 Hz)	1577, 1625, 1999,[d] 2068[d]
3	[D$_6$]DMSO	7.23 (9.16 Hz)	8.45 (9.16 Hz)	8.45 (9.16 Hz)	7.71 [R = H] (7.32 Hz)	1579, 1628, 3246,[e] 1385[f]
4	[D$_6$]DMSO	7.05 (9.16 Hz)	8.32 (9.80 Hz)	8.36 (7.92 Hz)	7.66 [R = H] (7.32 Hz)	1579, 1628
HL^2	$CDCl_3$	7.16 (9.16 Hz)	8.04 (9.16 Hz)	7.84	2.61 [R = CH_3]	1598, 1636
1b	$CDCl_3$	7.31 (9.16 Hz)	8.02 (9.16 Hz)	7.88	2.62 [R = CH_3]	1592, 1630, 1992,[d] 2061[d]
2a	[D$_7$]DMF[c]	7.35 (9.16 Hz)	8.20 (9.16 Hz)	7.77	2.61 [R = CH_3]	1594, 1630
HL^3	$CDCl_3$	7.16 (9.76 Hz)	8.06 (9.16 Hz)	7.84	0.99–2.86 [R = Pr]	1597, 1633
1c	$CDCl_3$	7.31 (9.16 Hz)	8.04 (9.16 Hz)	7.88	0.99–2.89 [R = Pr]	1593, 1631, 2004,[d] 2067[d]
2b	$CDCl_3$	7.45 (9.16 Hz)	7.93 (9.76 Hz)	7.85	0.98–2.86 [R = Pr]	1591, 1629

[a] Numbering of hydrogen is shown in Scheme 1. [b] KBr pellet. [c] Measured at 70 °C. [d] C≡O stretch. [e] N–H stretch. [f] N–O stretch.

Table 2. Crystallographic parameters for **1**–**4**.

	1a	**1b**	**2a**	**2b**	**3**	**4**
Empirical formula	$C_{15}H_7O_4Rh$	$C_{16}H_9O_4Rh$	$C_{28}H_{18}O_4Pd$	$C_{32}H_{26}O_4Pd$	$C_{13}H_{13}N_3O_5Pt$	$C_{29}H_{43}Cl_2NO_2Pt$
Formula weight	354.12	368.14	524.85	580.93	486.35	703.66
Crystal dimensions [mm]	0.5×0.25×0.25	0.1×0.02×0.9	0.2×0.13×0.04	0.4×0.1×0.08	0.5×0.25×0.25	0.4×0.3×0.3
Crystal system	monoclinic	monoclinic	monoclinic	monoclinic	monoclinic	monoclinic
a [Å]	9.9623(13)	9.1960(15)	7.4391(7)	7.5663(7)	11.525(2)	16.366(7)
b [Å]	4.5870(6)	10.0050(16)	8.5785(8)	9.7649(10)	5.916(1)	8.732(3)
c [Å]	14.3155(18)	15.178(2)	16.005(2)	16.4833(16)	10.528(2)	22.127(9)
β [°]	107.070(2)	107.407(3)	91.882(2)	100.641(2)	89.17(1)	116.303(6)
V [Å^3]	625.36(14)	1332.5(4)	1020.8(2)	1196.9(2)	717.8(2)	2834.8(18)
Space group	$P2_1$ (#4)	$P2_1/n$ (#14)	$P2_1/c$ (#14)	$P2_1/c$ (#14)	Pc (#7)	Cc (#9)
Z	2	4	2	2	2	4
$D_{calcd.}$ [g cm^{-3}]	1.881	1.835	1.707	1.612	2.250	1.649
μ [mm^{-1}]	1.374	1.294	0.946	0.814	9.763	5.145
F(000)	348	728	528	592	460	1408
No. of reflections	4634	9597	7661	8649	5363	12885
No. of observations	2768	3285	1837	2943	4714	5244
Diffractometer	Bruker APEX	Bruker APEX	Bruker APEX	Bruker APEX	Rigaku Mercury	Rigaku Mercury
Radiation	Mo-K_α	Mo-K_α	Mo-K_α	Mo-K_α	Mo-K_α	Mo-K_α
Refl./param. ratio	15.29	17.20	11.48	17.31	24.62	9.87
Temperature [K]	293	293	293	293	293	120
R_1, R_w[a]	0.0486, 0.1190	0.037; 0.069	0.030; 0.072	0.0353; 0.0775	0.046; 0.136	0.058; 0.147
Goodness of fit	1.01	1.05	1.11	1.06	1.14	1.01

[a] $R_1 = \Sigma||F_o| - |F_c||/\Sigma|F_o|$; $R_w = [\Sigma w(F_o^2 - F_c^2)^2/\Sigma w(F_o^2)^2]^{1/2}$.

1b were almost identical; the structure of **1b**, determined by X-ray crystallography, is shown in Figure 1. Comparing the intramolecular bond lengths of these complexes with those of [Rh^I(acac)(CO)$_2$] (acac = acetylacetone)[13] shows that the Rh–O and C≡O distances are shorter in the phenalenone complexes (by about 0.04 and 0.1 Å, respectively), while the Rh–C(CO) distances are longer (by about 0.09 Å). This suggests that the bonds between Rh and the chelating ligand are somewhat stronger in the phenalenone complexes.

The packing diagram of **1a** is shown in Figure 2. The crystal structure has a polar space group ($P2_1$), in which the molecules are arranged in a column along the stacking (*b*) axis. There is no intermolecular metal–metal bonding: the intermolecular Rh···Rh distance is 4.587 Å. The packing of **1b** is different from that of **1a** and is shown in Figure 3. An intermolecular Rh–Rh interaction [Rh–Rh: 3.2336(6) Å] forms dimers, which have a staggered configuration. In the crystal, the long molecular axes are located within the *a*–*c* plane, and interdimer face-to-face stacking interactions form columns along the *b* axis. The molecules in adjacent columns are arranged such that their long axes are orthogonal.

It is known that d^8 metal complexes can associate through metal–metal interactions in the solid state.[2a,18] In [Rh^I(acac)(CO)$_2$],[13] the molecules form one-dimensional arrays with Rh···Rh distances of 3.26 Å. The Rh–Rh distance in **1b** is comparable to that in Rh^I 1D chain complexes and bridged dinuclear Rh^I complexes.[19–21]

Solutions of **1a** and **1b** were yellow and exhibited almost identical absorption spectra, but **1b** formed intense deep red crystals while **1a** remained yellow in the crystalline state. Similar structure-dependent color change has been observed previously in some platinum complexes.[22] Figure 4 (a) and (b) show the absorption and emission spectra of powder samples of **1a** and **1b**, respectively. Solid lines represent room temperature absorption spectra, obtained by applying a Kubelka–Munk conversion to reflectance spectra. The absorption edge of **1a** appears at around 500 nm while that for **1b** appears at around 600 nm; the lower energy of **1b**'s absorption is consistent with its intense color. The broken lines in Figure 4 represent the emission spectra at 77 K. Compound **1a** exhibited red emission, with two bands at λ_{max} = 600 nm and λ_{max} = 648 nm. Compound **1b** exhibited a weak, broad band at λ_{max} = 658 nm. These complexes were emissive at 77 K but not room temperature, and not in solution.

The low-energy absorption in **1b** is a consequence of metal–metal interactions. DFT calculations were carried out using the crystallographically determined geometries of **1a** and **1b**, and the frontier orbitals are plotted in Figure 5. In **1a**, the HOMO (–6.22 eV) and LUMO (–2.69 eV) are of predominantly ligand character with only a small contribution from the metal d orbitals. The d orbitals' contribution is more significant for the HOMO and therefore the lowest energy excitation is predominantly π–π* mixed with an MLCT character. In contrast to **1a**, the HOMO of **1b** (–5.48 eV) consists of metal dz^2 orbitals; the d–d interaction raises the energy level of the Rh^I–Rh^I σ-antibonding orbital above that of the ligand orbital. The LUMO (–2.53 eV) is a ligand-based orbital. Therefore, the intense color of **1b** is attributed to MLCT. Electronic absorptions from metal-centered ($4d_{z^2}$ to $5p_z$) transitions in binuclear rhodium complexes are mostly found between 550 and 600 nm,[20] but the transition in **1b** is of a different character because the conjugation of the ligand lowers the π* level. The crystal structure of **1c** could not be determined but its yellow color suggests that it has no metal–metal interactions.

Table 3. Selected bond lengths [Å] and bond angles [°] with estimated standard deviations in parentheses.

1a			
Rh–O1	2.008(5)	Rh–O2	2.007(5)
Rh–C14	1.848(8)	Rh–C15	1.845(8)
O1–C1	1.285(8)	O2–C3	1.285(8)
C1–C2	1.434(8)	C1–C12	1.417(10)
C2–C3	1.428(8)	C3–C4	1.431(9)
C14–O4[a]	1.125(10)	C15–O3[a]	1.129(10)
O1–Rh–O2	88.8(2)	C14–Rh–C15	88.2(4)
O1–Rh–C14	92.1(3)	O2–Rh–C15	91.0(3)
C1–O1–Rh	128.9(4)	C3–O2–Rh	129.1(4)
C2–C1–O1	125.2(6)	C2–C3–O2	125.1(6)
1b			
Rh–O1	2.018(2)	Rh–O2	2.021(2)
Rh–C15	1.846(3)	Rh–C16	1.839(3)
O1–C1	1.290(3)	O2–C3	1.284(3)
C1–C2	1.431(3)	C1–C12	1.433(3)
C2–C3	1.425(3)	C3–C4	1.439(3)
C15–O4[a]	1.136(3)	C16–O3[a]	1.133(6)
O1–Rh–O2	89.00(6)	C15–Rh–C16	87.7(1)
O1–Rh–C15	91.97(9)	O2–Rh–C16	91.34(9)
C1–O1–Rh	128.0(1)	C3–O2–Rh	128.6(1)
C2–C1–O1	125.9(2)	C2–C3–O2	125.6(2)
2a			
Pd–O1	1.960(2)	Pd–O2	1.978(2)
O1–C1	1.293(4)	O2–C3	1.284(3)
C1–C2	1.421(4)	C1–C12	1.434(4)
C2–C3	1.440(4)	C3–C4	1.437(4)
O1–Pd–O2	93.38(8)	Pd–O1–C1	125.4(2)
Pd–O2–C3	125.4(2)	O1–C1–C2	126.6(3)
O2–C3–C2	126.1(3)	C1–C2–C3	122.9(3)
O1–C1–C12	114.8(3)	O2–C3–C4	115.6(3)
2b			
Pd–O1	1.965(1)	Pd–O2	1.972(1)
O1–C1	1.284(2)	O2–C3	1.289(2)
C1–C2	1.437(2)	C1–C12	1.432(3)
C2–C3	1.427(2)	C3–C4	1434(3)
O1–Pd–O2	93.67(6)	Pd–O1–C1	125.4(1)
Pd–O2–C3	125.2(1)	O1–C1–C2	126.1(2)
O2–C3–C2	126.1(2)	C1–C2–C3	123.4(2)
O1–C1–C12	115.5(2)	O2–C3–C4	115.3(2)
3			
Pt–N1	2.020(9)	Pt–N2	2.025(10)
Pt–O1	1.962(7)	Pt–O2	1.998(8)
O1–C1	1.31(1)	O2–C3	1.31(1)
C1–C2	1.42(1)	C2–C3	1.42(1)
C3–C4	1.43(1)	C1–C12	1.42(1)
N1–Pt–N2	92.3(3)	O1–Pt–O2	94.3(3)
O1–Pt–N1	86.6(3)	O2–Pt–N2	86.9(4)
C1–O1–Pt	124.1(6)	C3–O2–Pt	123.8(6)
C2–C1–O1	126.6(9)	C2–C3–O2	125.9(9)
4			
Pt–Cl1	2.284(5)	Pt–Cl2	2.300(5)
Pt–O1	1.961(13)	Pt–O2	1.975(10)
O1–C1	1.29(2)	O2–C3	1.30(2)
C1–C2	1.42(2)	C2–C3	1.44(2)
C3–C4	1.44(2)	C1–C12	1.46(2)
Cl1–Pt–Cl2	91.8(2)	O1–Pt–O2	93.7(5)
O1–Pt–Cl1	87.9(4)	O2–Pt–Cl2	86.8(3)
C1–O1–Pt	125.5(10)	C3–O2–Pt	124.5(8)
C2–C1–O1	126.5(13)	C2–C3–O2	126.2(11)

[a] Carbonyl groups (C≡O).

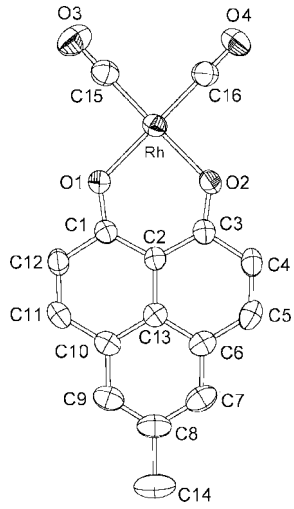

Figure 1. ORTEP drawing of the molecular structure of **1b** with the atom-numbering scheme. The counterions are omitted. Displacement ellipsoids are shown at the 50% probability level. The numbering of the phenalenyl moiety is the same in the other complexes.

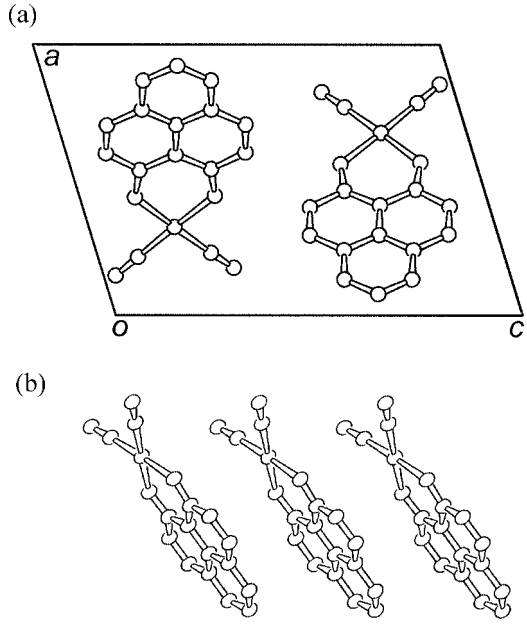

Figure 2. (a) Packing diagram of **1a** viewed along the *b* axis. (b) Stacking arrangement of **1a**.

Mononuclear Rh^I complexes are known to emit from MLCT or π–π* intraligand excited states.[23] The emission from **1a** is assigned to vibronic progressions from the π–π* excited state mixed with some MLCT character. Consistent with this, a long emission lifetime of 2.0 ms was observed for this band. Solid $[Rh^I(acac)_2(CO)_2]$ also exhibits weak π–π* emission as a structured band in the 430–530 region.[16] Dinuclear Rh^I complexes often exhibit a strong red emission between 650 and 850 nm because of metal–metal interactions,[21] but, in the case of **1b**, the emission was very weak. This might be a consequence of the highly conjugated nature of the ligand.

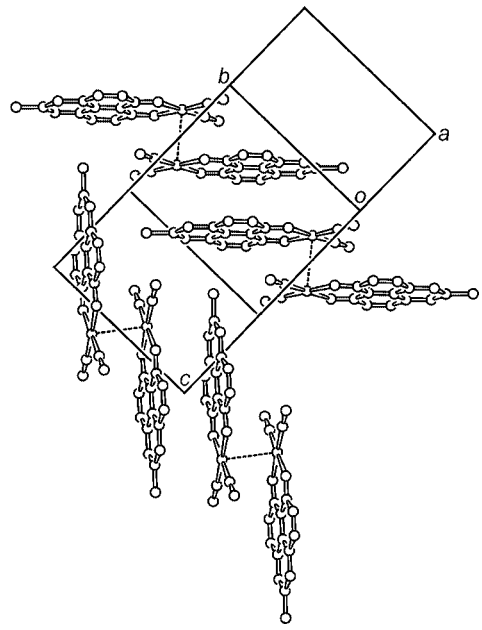

Figure 3. Packing diagram of **1b**. The hydrogen atoms are omitted for clarity. The dashed lines represent Rh–Rh interactions.

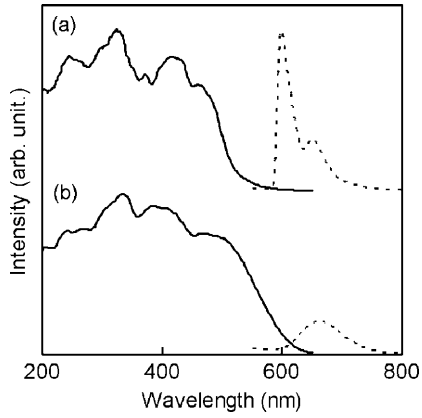

Figure 4. UV/Vis absorption spectra at room temperature (solid lines) and emission spectra at 77 K (dashed lines) for solid samples of (a) **1a** and (b) **1b**.

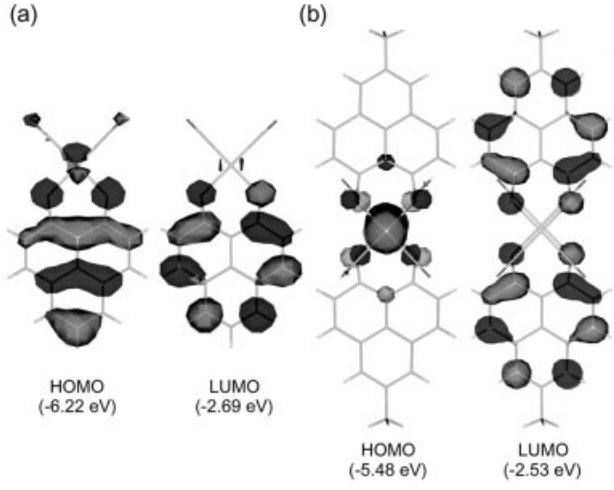

Figure 5. Frontier orbitals for (a) **1a** and (b) **1b** (dimer) derived from DFT calculations.

$[Pd^{II}(L^2)_2]$ (2a) and $[Pd^{II}(L^3)_2]$ (2b)

The molecular structures of **2a** and **2b**, determined by X-ray crystallography, are almost identical. The coordination of the palladium atom in each case is square planar, forming an extended π-conjugated planar complex. The Pd–O distances are comparable to those in the chelate complex $[Pd(acac)_2]$.[12] The packing diagram of **2a** is shown in Figure 6 (a), and the structure of **2b** is almost identical, except that the *b* axis is elongated (by 1.2 Å) because of the longer

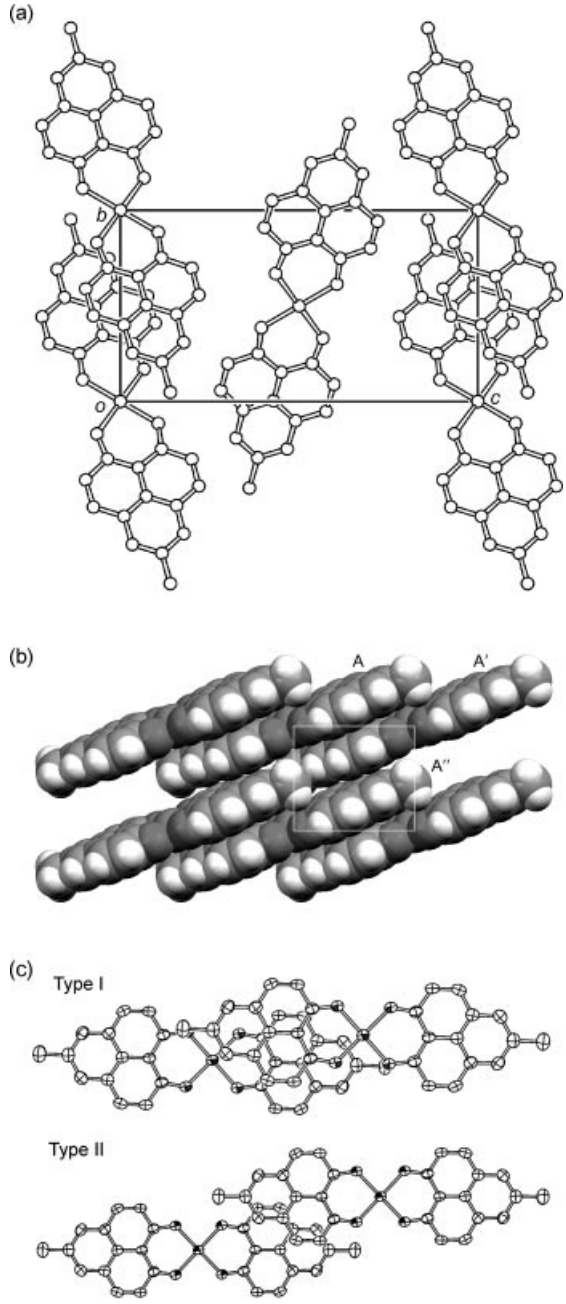

Figure 6. (a) Packing diagram of **2a** viewed along the *a* axis. The hydrogen atoms are omitted for clarity. (b) Space-filling representation of the sheet structure of **2a** within the *ab* plane. (c) ORTEP drawing of the overlapping modes of **2a**, viewed along the molecular plane.

alkyl group. The packing diagram of **2b** has been deposited as supporting information. In both crystals, the palladium atoms are located on the origin of the crystal lattice, and the closest distances between palladium atoms are equal to the *a* axis length: 7.439 Å for **2a** and 7.566 Å for **2b**. The complexes form two-dimensional layered structures, consisting of stacking of the planar molecules along the *a* axis. The layered structure of **2a** is shown in Figure 6 (b) as a space-filling model. There are two stacking modes, as shown in Figure 6 (c): type I stacking is formed between molecules A and A′ in Figure 6 (b), the symmetry code for A′ being x, $1 + y$, z, and type II stacking is formed between molecules A′ and A′′, the symmetry code for A′′ being $1 + x$, $1 + y$, z. The overlap between phenalenyl rings is larger for type I than type II. The stacking modes of **2a** and **2b** are similar, although the overlap of stacking type II is slightly more significant in **2b**, which results in stronger intermolecular interactions. It is interesting to note that the stacking structures of these complexes resemble those of polycyclic aromatic compounds.

$[Pt^{II}(L^1)(NH_3)_2](NO_3)$ (3) and $(Bu_4N)[Pt^{II}(L^1)(Cl)_2]$ (4)

Complex **3** shows an approximate C_{2v} structure. The distances C(1)–C(2), C(2)–C(3), and C(3)–C(4) are about 1.42 Å, and Pt–O(1) and Pt–O(2) are about 1.96 Å. These bond lengths are similar to the corresponding distances in the chelate compounds $[Pt(acac)_2]$[24] and $[PtCl_2(acac)]$.[14] Figure 7 shows the packing diagram. This complex has a layered structure, with hydrogen-bonded sheets and hydrophobic phenalenone layers arranged alternately along the *a* axis. The two ammine ligands are involved in intermolecular hydrogen bonding with the nitrate counteranions (N–H···O distances: 2.89 and 3.03 Å) to form a two-dimensional zigzag hydrogen-bond network within the *b*–*c* plane. Within the phenalenone layer, the aromatic rings have a herring-bone-like arrangement. Furthermore, this crystal has a polar space group (*Pc*), which is associated with a hydrogen-bond-assisted arrangement of the phenalenone complex, as seen in Figure 7. The face-to-face distance between the neighboring phenalenone planes along the *b* axis is 4.5 Å. The intermolecular distance between the neighboring platinum atoms is 5.9 Å; no direct metal–metal interactions are observed.

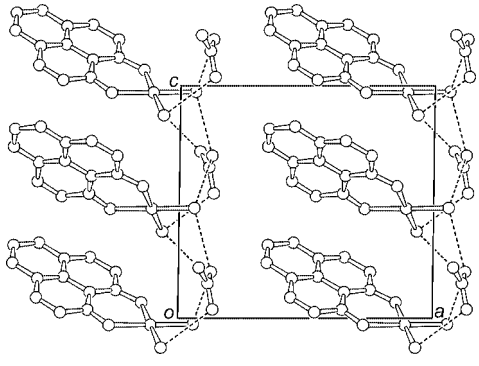

Figure 7. Packing diagram of **3** viewed along the *b* axis. The hydrogen atoms are omitted for clarity. The dashed lines represent hydrogen bonds.

In complex **4**, the lengths of the C–C and Pt–O bonds are almost the same as those found in **3**. The Pt–Cl distances are about 2.30 Å, which is comparable to the value found in $[PtCl_2(acac)]$.[14] The tetrabutyl ammonium cation and phenalenone complex anion are paired and arranged alternately in the crystal. The distance between neighboring platinum atoms is 8.73 Å; again, there were no metal–metal interactions. The molecular structure and packing diagram of **4** are deposited as Supporting Information.

Cytotoxic Activities

Antitumor activity, as typified by cisplatin (*cis*-$[PtCl_2(NH_3)_2]$), is an important feature of platinum-group metal complexes.[25] In this study, we have evaluated the cytotoxic activities of **1a**, **3**, and **4** against human acute myeloid leukemia (HL60) cells. The concentration of the metal complexes giving a growth inhibition of 50% (IC_{50}) was evaluated in vitro by the MTT assay. The IC_{50} values (estimated standard deviations) for **1a**, **3**, and **4** were 3.12 (0.37), 1.69 (0.51), and 3.62 (0.46) μmol/L, respectively. The observed activities were of the same order, although **3** seems to be somewhat more active than the others. Under the same experimental conditions, the IC_{50} for cisplatin was 3.16 (0.50) μmol/L (control for **1a**) and 2.19 (0.59) μmol/L (control for **3** and **4**). Thus, the present compounds have the same order of cytotoxic activity as cisplatin. However, the activity is possibly due to the ligand, and, therefore, the cytotoxicity of 9-hydroxyphenalenone needs to be evaluated for discussion of the cytotoxicity of the metal complexes.

Conclusions

We have prepared a series of platinum-group metal complexes with hydroxyphenalenone derivatives and investigated their structures, properties, and cytotoxic activities. In the solid state, the colors of the rhodium complexes **1a** and **1b** are very different; we attribute the intense color of the latter to metal–metal interactions. These compounds were emissive at 77 K in the solid state, but the highly conjugated ligands might not be favorable for emission. In the crystals of these rhodium complexes, change of ligand led to a different packing arrangement, but no corresponding change in packing was seen in the palladium complexes **2a** and **2b**. Complexes **2a** and **2b** exhibited interesting packing arrangements. No metal–metal interactions were seen in these complexes, but incorporation of a sterically hindered substituent at the 5-position of the ligand might lead to a staggered molecular arrangement and shortened metal–metal distances. The rhodium and platinum complexes exhibit noteworthy cytotoxic activity. Future research into phenalenone complexes might focus on the construction of one-dimensional complexes with metal–metal interactions, and, furthermore, use a redoxed ligand (that is, a phenalenyl radical), which could interact with the one-dimensional electronic system.

Experimental Section

General Remarks: NMR spectra were recorded with a JEOL JNM-ECL-400 spectrometer. Infrared spectra were recorded as KBr pellets on a JASCO FTIR 230 spectrometer. UV/Vis spectra were recorded with a JASCO V-570 UV/Vis/NIR spectrometer. Solid-state electronic absorption spectra were measured with the same spectrometer equipped with an integrating sphere for diffuse reflectance spectroscopy, Kubelka–Munk conversion being applied to the resultant spectra. Emission spectra were recorded with a JASCO FP-6500 spectrometer. DFT calculations were performed with Gaussian 98[26] software at the B3LYP level using a Lanl2DZ basis set.

Cytotoxic Studies: The direct growth-inhibition effects of **1a**, **3**, and **4** were examined in vitro against HL60 human acute myeloid leukemia cells. These cells were obtained from the RIKEN Cell Bank, Japan. The HL60 cells were washed and suspended in the culture medium at a concentration of 3×10^4 cells/mL, and this suspension was incubated in 5% CO_2/air for 24 h at 37 °C. To this suspension was added the metal complex dissolved in ethanol and water. Cisplatin was used as control. These cells were further incubated for 72 h, and cell growth evaluated using a modified 3-(4,5-dimethylthiazol-2-yl)-2,5-diphenyltetrazolium bromide (MTT) reduction assay.[27] After termination of the cell culture, MTT in phosphate-buffered saline was added to each well and incubated for 4 h in 5% CO_2/air at 37 °C. After adding DMSO, the plates were examined using a microplate reader at 550 nm.

X-ray Crystallographic Study: X-ray diffraction data for single crystals were collected on a Rigaku Mercury or a Bruker APEX CCD diffractometer using Mo-K_α radiation (λ = 0.71073 Å). The structures were solved by the direct method (SHELXS 97[28]) and expanded using Fourier techniques. The non-hydrogen atoms were refined anisotropically. Hydrogen atoms were inserted at the calculated positions and allowed to ride on their respective parent atoms.

CCDC-259428 (for **1a**), -259427 (for **1b**), -259429 (for **2a**), -259430 (for **2b**), -259431 (for **3**), and -259432 (for **4**) contain the supplementary crystallographic data for this paper. These data can be obtained free of charge from The Cambridge Crystallographic Data Centre via www.ccdc.cam.ac.uk/data_request/cif.

Ligands: The syntheses of 9-hydroxyphenalenone (HL^1) and 9-hydroxy-5-methylphenalenone (HL^2) were carried out according to published methods,[29] and 9-hydroxy-5-propylphenalenone (HL^3) was prepared from 6-methoxy-2-propylnaphthalene[30] in the same way as HL^2. The crude product was purified by sublimation under vacuum followed by recrystallization from hexane to give a yield of 44%.

$[Rh^I(L^1)(CO)_2]$ (1a): To a stirred DMF solution (1 mL) of $[Rh(CO)_2Cl]_2$ (15 mg, 3.9×10^{-5} mol), which was cooled in an ice bath, 9-hydroxyphenalenone (HL^1) (16 mg, 8.1×10^{-5} mol) was added, dissolved in a methanol solution of potassium hydroxide (9.3×10^{-5} mol). A lustrous red powder precipitated immediately, which was collected by filtration, washed with dichloromethane, and dried under vacuum to afford a yellow powder; 57% yield (16 mg). Yellow plate-like crystals suitable for X-ray crystallography were obtained by recrystallization from dichloromethane/pentane. λ_{max}/nm (DMF): 266, 352, 368, 428, 452. $C_{15}H_7O_4Rh$ (354.11): calcd. C 50.88, H 1.99; found: C 50.62, H 2.13.

$[Rh^I(L^2)(CO)_2]$ (1b): This compound was prepared in the same way as **1a**, using 15 mg (8.5×10^{-5} mol) of 9-hydroxy-5-methylphenalenone (HL^2). Red powder, 84% yield (24 mg). Red needle-like crystals suitable for X-ray crystallography were obtained by recrystallization from dichloromethane/hexane. λ_{max}/nm (DMF): 266, 356, 372, 436, 462. $C_{32}H_{18}O_8Rh_2$ (736.26): calcd. C 52.20, H 2.46; found C 51.92, H 2.60.

$[Rh^I(L^3)(CO)_2]$ (1c): This compound was prepared in the same way as **1a**, using $[Rh(CO)_2Cl_2]$ (22 mg, (5.7×10^{-5} mol), 9-hydroxy-5-propylphenalenone (HL^2) (26 mg, 1.1×10^{-4} mol), and potassium hydroxide in methanol (1.0×10^{-4} mol), and stirring for 30 min. A yellow powder was obtained in a quantitative yield. λ_{max}/nm (CH_2Cl_2): 369, 435, 462. $C_{18}H_{13}O_4Rh$ (396.18): calcd. C 54.57, H 3.31; found C 54.75, H 3.56.

$[Pd^{II}(L^2)_2]$ (2a): 9-Hydroxy-5-methylphenalenone (HL^2) (22 mg, 1.1×10^{-4} mol) and a methanol solution of potassium hydroxide (1.6×10^{-4} mol) were added to a stirred aqueous solution (1 mL) of K_2PdCl_4 (15 mg, 4.6×10^{-5} mol). An orange precipitate was generated immediately, which was collected by filtration, washed with dichloromethane, and dried under vacuum. Orange needles, 92% yield (22 mg). Single crystals suitable for X-ray crystallography were obtained by slow cooling of a hot DMF solution. λ_{max}/nm (DMF): 367, 385, 498. $C_{28}H_{18}O_4Pd$ (524.82): calcd. C 64.07, H 3.46; found C 62.13, H 3.62.

$[Pd^{II}(L^3)_2]$ (2b): This compound was prepared in the same way as **2a**, using K_2PdCl_4 (16 mg, 4.8×10^{-5} mol), 9-hydroxy-5-propylphenalenone (HL^3) (22 mg, 9.2×10^{-5} mol), and potassium hydroxide (1.2×10^{-4} mol), and heating for 30 min at 50 °C. Red-orange powder, 80% yield (22 mg). Single crystals were obtained by recrystallization from DMF. λ_{max}/nm (DMF): 271, 369, 384, 466, 497. $C_{32}H_{26}O_4Pd$ (580.93): calcd. C 66.16, H 4.51; found C 65.94, H 4.59.

$[Pt^{II}(L^1)(NH_3)_2](NO_3)$ (3): Silver nitrate (44 mg, 2.6×10^{-4} mol) was added to a solution of *cis*-$Pt(NH_3)_2Cl_2$ (40 mg, 1.3×10^{-4} mol) in methanol/water (1:3 v/v, 1 mL) . This solution was stirred in the dark at 60 °C for 3 h, and then the AgCl was removed by filtration (Celite plug). 9-Hydroxyphenalenone (HL^1) (26 mg, 1.3×10^{-4} mol) and a methanol solution of potassium hydroxide (1.3×10^{-4} mol) were added to this solution of *cis*-$[Pt(NH_3)_2(H_2O)_2](NO_3)_2$. After stirring for 3 h at 60 °C, the solvent was removed by vacuum evaporation. Orange powder, 54% yield (31 mg). Orange needle-like crystals suitable for X-ray crystallography were obtained by recrystallization from DMF/diethyl ether. λ_{max}/nm (DMF): 378, 395, 452, 477. $C_{13}H_{13}N_3O_5Pt$ (486.36): calcd. C 32.11, H 2.69, N 8.64; found C 31.95, H 2.72, N 8.71.

$(Bu_4N)[Pt^{II}(L^1)(Cl)_2]$ (4): A 10% tetrabutylammonium hydroxide/methanol solution (250 mg, 9.6×10^{-4} mol) was added to a stirred methanol solution (0.3 mL) of 9-hydroxyphenalenone (HL^1) (9.7 mg, 4.9×10^{-5} mol). This solution was transferred to a test tube, and a methanol solution (2 mL) of K_2PtCl_4 (20 mg, 4.8×10^{-5} mol) and 18-crown-6 (60 mg, 2.3×10^{-5} mol) was layered over the solution and allowed to react slowly by diffusion. Over a few days, the color of the solution changed from orange to red, and a black powder was gradually deposited. The powder was removed by filtration, and the filtrate concentrated to a small volume on a rotary evaporator. After adding a small amount of water, the solution was cooled in an ice bath for about 1 h. A red powder precipitated, which was collected by filtration, washed with dichloromethane, and dried under vacuum. Red powder, 26% yield (8.8 mg). Needle-like crystals suitable for X-ray crystallography were obtained by recrystallization from DMF/diethyl ether. λ_{max}/nm (DMF): 350, 414, 438, 461. $C_{29}H_{43}Cl_2NO_2Pt$ (703.64): calcd. C 49.50, H 6.16, N 1.99; found C 48.95, H 6.07, N 2.06.

Supporting Information: (see footnote on the first page of this article) ORTEP drawings of the molecular structures of **1a**, **2a**, **3**, and **4**, and packing diagrams of **2b** and **4** are provided.

Acknowledgments

This work was financially supported by "High-Tech Research Center" Project 2005–2009 from MEXT (Ministry of Education, Culture, Sports, Science and Technology). We thank Dr. Mikio Ueda (Toho University) for helpful suggestions on the preparations, Mr. Kazuya Okazawa (Toho University) for crystallographic analyses, and Ms. Ayako Morishima (JASCO Corp.) for measuring emission spectra. We also thank the Japan Science and Technology Agency for the loan of experimental equipment. Mr. Masaru Nakama (Warpstream, Tokyo) is also acknowledged for providing Web-DB systems. This work was performed using the facilities of the Institute for Solid State Physics at the University of Tokyo.

[1] a) V. W.-W. Yam, C.-K. Hui, K. M.-C. Wong, N. Zhu, K.-K. Cheung, *Organometallics* **2002**, *21*, 4326–4334, and references cited therein; b) J. Brooks, Y. Babayan, S. Lamansky, P. I. Djurovich, I. Tsyba, R. Ban, M. E. Thompson, *Inorg. Chem.* **2002**, *41*, 3055–3066, and references cited therein; c) A. J. Lees, *Chem. Rev.* **1987**, *87*, 711–743; d) D. M. Roundhill, *Photochemistry and Photophysics of Metal Complexes*, Plenum Press, New York, **1994**; e) M. Hissler, J. E. McGarrah, W. B. Connick, D. K. Geiger, S. D. Cummings, R. Eisenberg, *Coord. Chem. Rev.* **2000**, *208*, 115–137; f) A. Vogler, H. Kunkely, *Top. Curr. Chem.* **2001**, *213*, 143–182; g) G. L. Geoffroy, M. S. Wrighton, *Organometallic Photochemistry*, Academic Press, New York, **1979**.

[2] a) *Extended Linear Chain Compounds* (Ed.: J. S. Miller), vols. 1–3, Plenum Press, New York, **1982**–**1983**; b) K. Sakai, M. Takeshita, Y. Tanaka, T. Ue, M. Yanagisawa, M. Kosaka, T. Tsubomura, M. Ato, T. Nakano, *J. Am. Chem. Soc.* **1998**, *120*, 11353–11363; c) M. E. Prater, L. E. Pence, R. Clérac, G. M. Finniss, C. Campana, P. A. Senzier, D. Jérome, E. Canadell, K. R. Dunbar, *J. Am. Chem. Soc.* **1999**, *121*, 8005–8016; d) M. Kato, A. Omura, A. Toshikawa, S. Kishi, Y. Sugimoto, *Angew. Chem. Int. Ed.* **2002**, *41*, 3183–3185; e) H. Kishida, H. Matsuzaki, H. Okamoto, T. Manabe, M. Yamashita, Y. Taguchi, Y. Tokura, *Nature* **2000**, *405*, 929–932.

[3] R. C. Haddon, *Nature* **1975**, *256*, 394–396.

[4] K. Goto, T. Kubo, K. Yamamoto, K. Nakasuji, K. Sato, D. Shiomi, T. Takui, M. Kubota, T. Kobayashi, K. Yakushi, J. Ouyang, *J. Am. Chem. Soc.* **1999**, *121*, 1619–1620.

[5] a) M. E. Etkis, X. Chi, A. W. Cordes, R. C. Haddon, *Science* **2002**, *296*, 1443–1445; b) X. Chi, M. E. Itkis, K. Kirschbaum, A. A. Pinkerton, R. T. Oakley, A. W. Cordes, R. C. Haddon, *J. Am. Chem. Soc.* **2001**, *123*, 4041–4048.

[6] K. Nakasuji, M. Yamaguchi, I. Murata, *Chem. Lett.* **1983**, 1489–1490.

[7] a) R. Neidlein, Z. Behzadi, *Chem. Ztg.* **1976**, *100*, 388–389; b) R. Neidlein, Z. Behzadi, *Chem. Ztg.* **1978**, *102*, 150–152.

[8] Y. Demura, T. Kawato, H. Kanatomi, I. Murase, *Bull. Chem. Soc. Jpn.* **1975**, *48*, 2820–2824.

[9] R. C. Haddon, United States Patent, **2002**, 6,428,912.

[10] R. V. Deun, P. Nockemann, P. Fias, K. V. Hecke, L. V. Meervelt, K. Binnemans, *Chem. Commun.* **2005**, 590–592.

[11] a) A. Werner, *Ber. Dtsch. Chem. Ges.* **1901**, *34*, 2584–2593; b) G. T. Behnke, K. Nakamoto, *Inorg. Chem.* **1967**, *6*, 433–440.

[12] S. Okeya, S. Ooi, K. Matsumoto, Y. Nakamura, S. Kawaguchi, *Bull. Chem. Soc. Jpn.* **1981**, *54*, 1085–1095.

[13] N. A. Bailey, E. Coates, G. B. Robertson, F. Bonati, R. Ugo, *J. Chem. Soc., Chem. Commun.* **1967**, 1041–1042.

[14] G. T. Behnke, K. Nakamoto, *Inorg. Chem.* **1967**, *6*, 433–440.

[15] J. Conradie, G. J. Lamprecht, S. Otto, J. C. Swarts, *Inorg. Chim. Acta* **2002**, *328*, 191–203.

[16] N. Dunwoody, S.-S. Sun, A. J. Lees, *Inorg. Chem.* **2000**, *39*, 4442–4451.

[17] ORTEP-3 for Windows, L. J. Farrugia, *J. Appl. Crystallogr.* **1997**, *30*, 565.

[18] J. S. Miller, A. J. Epstein, *Prog. Inorg. Chem.* **1976**, *20*, 1–151.

[19] a) J. Real, J. C. Bayón, F. J. Lahoz, J. A. López, *J. Chem. Soc., Chem. Commun.* **1989**, 1889–1890; b) C. W. Lange, M. Földeàki, V. I. Nevodchikov, V. K. Cherkasov, G. A. Abakumov, C. G. Pierpont, *J. Am. Chem. Soc.* **1992**, *114*, 4220–4222.

[20] a) O. Gerlits, A. U. Kovalevsky, P. Coppens, *Dalton Trans.* **2004**, 3955–3962; b) M. Inga, S. Kenney, J. W. Kenney, G. A. Crosby, *Organometallics* **1986**, *5*, 230–234; c) K. R. Mann, N. S. Lewis, R. M. Williams, H. B. Gray, J. G. Gordon II, *Inorg. Chem.* **1978**, *17*, 828–834; d) A. L. Balch, *J. Am. Chem. Soc.* **1976**, *98*, 8049–8054.

[21] a) C.-M. Che, W.-M. Lee, H.-L. Kwong, V. W.-W. Yam, K.-C. Cho, *J. Chem. Soc., Dalton Trans.* **1990**, 1717–1722; b) V. M. Miskowski, G. L. Nobinger, D. S. Kliger, G. S. Hammond, N. S. Lewis, K. R. Mann, H. B. Gray, *J. Am. Chem. Soc.* **1978**, *100*, 485–488; c) K. R. Mann, J. A. Thich, R. A. Bell, C. L. Coyle, H. B. Gray, *Inorg. Chem.* **1980**, *19*, 2462–2468; d) S. J. Milder, R. A. Goldbeck, D. S. Kliger, H. B. Gray, *J. Am. Chem. Soc.* **1980**, *102*, 6761–6764; e) W. A. Fordyce, G. A. Crosby, *J. Am. Chem. Soc.* **1982**, *104*, 985–988.

[22] C.-M. Che, L.-Y. He, C.-K. Poon, T. C. W. Mak, *Inorg. Chem.* **1989**, *28*, 3081–3083.

[23] G. L. Geoffroy, M. S. Wrighton, G. S. Hammond, H. B. Gray, *J. Am. Chem. Soc.* **1974**, *96*, 3105–3108.

[24] M. Katoh, K. Miki, Y. Kai, N. Tanaka, N. Kasai, *Bull. Chem. Soc. Jpn.* **1981**, *54*, 611–612.

[25] a) J. Reedijk, *Chem. Rev.* **1999**, *99*, 2499–2510; b) R. R. Jamieson, S. J. Lippard, *Chem. Rev.* **1999**, *99*, 2467–2498; c) B. Rosenberg, L. Van Camp, J. E. Trosko, V. H. Mansour, *Nature* **1969**, *222*, 385–386.

[26] *Gaussian 98, Revision A.11*, M. J. Frisch, G. W. Trucks, H. B. Schlegel, G. E. Scuseria, M. A. Robb, J. R. Cheeseman, V. G. Zakrzewski, J. A. Montgomery, Jr., R. E. Stratmann, J. C. Burant, S. Dapprich, J. M. Millam, A. D. Daniels, K. N. Kudin, M. C. Strain, O. Farkas, J. Tomasi, V. Barone, M. Cossi, R. Cammi, B. Mennucci, C. Pomelli, C. Adamo, S. Clifford, J. Ochterski, G. A. Petersson, P. Y. Ayala, Q. Cui, K. Morokuma, P. Salvador, J. J. Dannenberg, D. K. Malick, A. D. Rabuck, K. Raghavachari, J. B. Foresman, J. Cioslowski, J. V. Ortiz, A. G. Baboul, B. B. Stefanov, G. Liu, A. Liashenko, P. Piskorz, I. Komaromi, R. Gomperts, R. L. Martin, D. J. Fox, T. Keith, M. A. Al-Laham, C. Y. Peng, A. Nanayakkara, M. Challacombe, P. M. W. Gill, B. Johnson, W. Chen, M. W. Wong, J. L. Andres, C. Gonzalez, M. Head-Gordon, E. S. Replogle, J. A. Pople, Gaussian, Inc., Pittsburgh, **2001**.

[27] J. M. Sargent, C. G. Taylor, *Br. J. Cancer* **1989**, *60*, 206–210.

[28] G. M. Sheldrick, *Program for the Solution for Crystal Structures*, University of Göttingen, Germany, **1997**.

[29] R. C. Haddon, R. Rayford, A. M. Hirani, *J. Org. Chem.* **1981**, *46*, 4587–4588.

[30] N. G. Buu-Hoi, D. Labit, *J. Org. Chem.* **1957**, *22*, 912–914.

Received: September 3, 2005
Published Online: December 13, 2005

